The impact of health education and public sanitation on the spread of COVID-19

Xiaxia Kang[a], Fang Cheng[*,b]

[a]*Department of Mathematics, Lvliang University, Lishi 033000, China*
[b]*School of Statistics and Applied Mathematics, Anhui University of Finance & Economics, Bengbu, 233030, China*

Abstract

In this paper, we formulate a deterministic mathematical model SEAIRB to study the dynamics behavior of COVID-19 pandemic. The model incorporates the impact of two strategies, health education and public sanitation, on the spread of the epidemic. Firstly, by using Routh-Hurwitz criteria, the disease-free equilibrium is locally asymptotically stable when the basic reproduction number does not exceed 1. Further, by using the comparison theorem, the global asymptotic stability of the disease-free equilibrium is obtained. Finally, numerical simulations are performed to verify the theoretical analysis and analyze the impact of different control strategies on the spread of the epidemic.

Key words:
COVID-19; Health education; Sanitation; Global dynamic behavior.
AMS Subject Classification: 37B25; 37G10; 37N25.

1. Introduction

As early as March 2020, the COVID-19 epidemic had been basically under control in China. The reason why China successfully fights COVID-19 is due to the timely intervention measures of the government, such as city closure, tracking report on social isolation, improving public health and health education. Besides, some research results on COVID-19 are important for our country and even the world to fight against the pandemic [1, 2].

Many scholars have tried to study and analyze the epidemic situation of COVID-19 through dynamic model [3, 4]. Because mathematical models can not only help us understand the spread of infectious diseases, but also guide us to find the most effective strategy to eliminate the disease. So far, many effective results have been achieved in the study of the transimission dynamics of COVID-19 [5, 6]. Chen et al. put forward a Bats-Hosts-Reservoir-People transmission network model to caculate the transmissibility of COVID-19 virus and found that the R_0 of SARS CoV-2 from reservoir to person was lower than that of person to

*Corresponding author. Email: fcheng@aufe.edu.cn
Email addresses: kxx_math@163.com (Xiaxia Kang), fcheng@aufe.edu.cn (Fang Cheng)
April 9, 2023

person [7]. Tang et al. employed a general SEIR-type epidemiological model to assess the impact of public health interventions on infection and show that intensive contact tracking and isolation measures can effectively reduce the transmission risk of COVID-19 virus [1]. Sasmita et al. adopted a SEI2RS model considering five control strategies for predicting the peak of COVID-19 and concludes that the scenario consisting of large-scale social restriction, contact tracing, case detection and treatment, and the wearing of face masks, is the most rational scenario to control COVID-19 spreading in Indonesia [2]. The COVID-19 model proposed by Ndairou et al. focused on the transmission of super-spreaders individuals [4]. In addition, many scholars have analyzed the transmission pathway of COVID-19, the structural dynamics of the SARS-CoV-2 spike protein and its interactions with receptors at the atomistic and molecular scales from different perspectives [8, 9, 10, 11].

According to the research results received, we realized that the virus can not only be transmitted from person to person through sneezing, coughing or close contact droplets of infected person [12]. But it also can be indirectly transmitted through some enclosed spaces or inadequate ventilation places where positive patients have stayed [6, 8, 13, 14]. Especially, some patients with the new coronavirus do not have any symptoms of infection, and can can transmit new coronavirus [15, 16]. And studies has show that some close contacts may also spread the new coronavirus before being quarantined [16]. Some scholars have incorporateed the infectivity of asymptomatic infected people and close contacts into their models. However, few literatures focused on the indirect transmission of the virus in these two groups, and the impact of the health education and public health system on the spread of the epidemic. Thus, based on the classic SEIR model, we introduce two extra compartments, B and A, and then proposed a SEAIRB model to depict the spread of new coronavirus in the population and environment. Here, $B(t)$ and $A(t)$ represents the number of new coronavirus in aerosols or the environment and the number of asymptomatic infectious, respectively. Our main purpose is to explore the role health education, sanitation and treatment on COVID-19 control and elimination. Further, we analyse the global dynamics behavior of the system. Finally, we perform the sensitivity analysis of the basic reproduction number and the endemic equilibrium, and found that reducing the contact of exposed and susceptible persons are the most critical factor in achieving disease control.

2. Model formation

In this section, we formulate a new deterministic mathematical model SEAIRB that study the dynamic behavior of the transmission of COVID-19 pandemic. At any time instant t, the total population denoted $N(t)$ is divided into five time-dependent classes, namely Susceptible $S(t)$, close contacts $E(t)$, asymptomatic infectious $A(t)$, infectious $I(t)$ and Recovered $R(t)$. In addition, considering the phenomenon that asymptomatic infected individuals and close contacts go to supermarkets, shopping malls and other public places before diagnosis or quarantine, we incorporate an additional compartment, $B(t)$, which indicates the indirect transmission of the virus in the environment is considered. The detailed flow diagram of the model is presented in Figure 1.

Λ symbolizes the migration rate of susceptible individuals at a constant. Susceptible

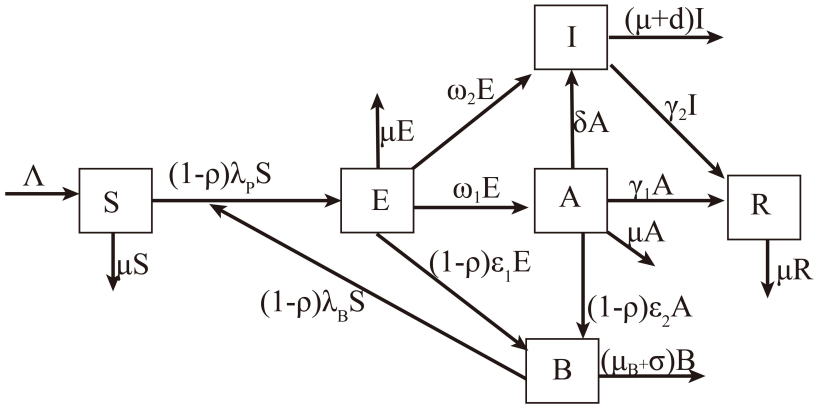

Figure 1: Flow diagram of the COVID-19 model with health education and sanitation.

individuals may acquire COVID-19 virus infectious following effective direct contact with close contacts, asymptomatic infectious individuals and infectious individuals at the time-dependent rate $\lambda_P(t)$ or after contacting contaminated environment at the time-dependent rate $\lambda_B(t)$. Here, $\lambda_P(t)$ represents direct transmission between human, the force of infection is given by $\lambda_P(t) = (1-\rho)(\beta_1 E(t) + \beta_2 A(t) + \beta_3 I(t))$ and $\lambda_B(t) = \frac{(1-\rho)\beta_4 B(t)}{K+B(t)}$. β_1, β_2 and β_3 is the transmission rate for close contacts, asymptomatic infectious and symptomatic infectious, respectively. K is the half-saturation constant of COVID-19 virus number in environment that yields a 50% chance of infect the disease. β_4 is the contact rate of Virus by individuals. $\frac{B}{K+B}$ represents the probability of a susceptible individual to develop coronavirus pneumonia per contact. It is assumed that health education has an effect of reducing the infection rate. Thus, the total transmission will be reduced by the rate $1-\rho$, where $\rho \in [0, 1)$ describe the efficacy of health education. $\rho = 0$, it means that health education has been ignored. When $\rho = 1$, it implies that education is 100% efficient in controlling the spread of COVID-19. Close contacts may either join infectious or symptomatic infectious. Close contacts may progress to infectious at the rate ω_1 and asymptomatic infectious at the rate ω_2.

Considering that there are some cases of asymptomatic infectious individuals showing symptoms in the isolation period. Therefore, we assumed that asymptomatic infectious individuals are screened at the rate δ and join the infectious individuals where they are finally treated at the rate γ_1. Symptomatic infectious individuals are treated at the rate γ_2. COVID-19 induced mortality rate for infectious individuals is denoted by d, while the natural death rate of humans is represented by μ. Infected individuals from both states $E(t)$ and $A(t)$ transmit COVID-19 virus into the environment at the rates $(1-\rho)\varepsilon_1$ and $(1-\rho)\varepsilon_2$, respectively. We assumed that the rate of excretion by the close contacts and asymptomatic infectious, ε_1 and ε_2, respectively. Here, we did not consider that symptomatic infectious individuals may spread virus into the environment. Because symptomatic infections in our country are isolated in time. It is worth noting that virus excretion of the asymptomatic

Table 1: Summary of some parameters for COVID-19 model.

Parameter	Description	Value
Λ	The input rate of susceptible individuals	20
β_1	Successful contact rate from close contacts	0.0001
β_2	Successful contact rate from asymptomatic infectious	0.0002
β_3	Successful contact rate from symptomatic infectious	0.00008
β_4	Effective transmission rate of virus due to environment to individuals	0.06
ω_1	Rate at which close contacts become asymptomatic infectious	0.1
ω_2	Rate at which close contacts become asymptomatic infectious	0.3
μ	Natural mortality rate	0.004
γ_1	Recovery rate of asymptomatic infected individuals	0.6
γ_2	Recovery rate of symptomatic infected individuals	0.1
d	Disease-induced death rate	0.06
δ	Transition rate of asymptomatic infected individuals to $I(t)$	0.3
ρ	Health education efficacy parameter	0.6
K	Half-saturation rate of virus that can cause a 50% chance of infections	1000
μ_B	Mortality rate of virus	0.1
ε_1	Virus shed into environment supply by close contacts	0.5
ε_2	Virus shed into environment supply by close contacts	0.3
σ	The death rate of virus due to sanitation	3

infectious and close contacts is low. However, COVID-19 virus in environment has an important role on the infection dynamics of COVID-19 due to its long duration and strong survival rate. we note that the new coronavirus does not reproduce independently in the aerosol. Thus, virus in the environment deplete naturally at μ_B or by sanitation measures at the rate σ. All parameters and their values in the model are presented in Table 1.

According to the schematic diagram in Figure 1, the differential equations of the mathematical model are

$$\begin{cases} \frac{\mathrm{d}S(\mathrm{t})}{\mathrm{dt}} = \Lambda - (1-\rho)(\beta_1 E + \beta_2 A + \beta_3 I + \frac{\beta_4 B}{K+B})S - \mu S, \\ \frac{\mathrm{d}E(\mathrm{t})}{\mathrm{dt}} = (1-\rho)(\beta_1 E + \beta_2 A + \beta_3 I + \frac{\beta_4 B}{K+B})S - (\mu + \omega_1 + \omega_2)E, \\ \frac{\mathrm{d}A(\mathrm{t})}{\mathrm{dt}} = \omega_1 E - (\mu + \delta + \gamma_1)A, \\ \frac{\mathrm{d}I(\mathrm{t})}{\mathrm{dt}} = \omega_2 E + \delta A - (\mu + d + \gamma_2)I, \\ \frac{\mathrm{d}R(\mathrm{t})}{\mathrm{dt}} = \gamma_1 A + \gamma_2 I - \mu R, \\ \frac{\mathrm{d}B(\mathrm{t})}{\mathrm{dt}} = (1-\rho)\varepsilon_1 E + (1-\rho)\varepsilon_2 A - (\mu_B + \sigma)B, \end{cases} \tag{2.1}$$

where the initial conditions $S(0) > 0, E(0) > 0, A(0) > 0,\ I(0) > 0,\ R(0) > 0, B(0) > 0$. Then, the system (2.1) has a biological invariant region as

$$\Omega = \left\{ S, E, A, I, R, B) \geq 0 : S + E + I + C + R \leq \frac{\Lambda}{\mu}, B \leq \frac{(1-\rho)(\varepsilon_1 + \varepsilon_2)\Lambda}{(\mu_B + \sigma)\mu} \right\},$$

where the parameter $\lambda > 0$ is the comprehensive input rate and $\mu > 0$ represents the

natural death rate. $d > 0$ denotes the death rate due to disease. In our model, the vertical transmission is not considered, i.e. all newborns are susceptible. According to the results of clinical practice, asymptomatic infections generally do not need treatment, but this group of people is a strong source of infection. Therefore, the incidence rate is where indicates the effective per captia contact rate of asymptomatic infections. Some asymptomatic infected people in the 14 day isolation period, will show obvious symptoms of infection, that is, diagnosed. The parameter p_1 is the rate at which the asymptomatic individuals become symptomatic individuals. If the asymptomatic infected person is asymptomatic during the 14 day isolation period and the nucleic acid test is negative for two times, the isolation can be released. We hypothesized that the asymptomatic infected patients who were released from isolation were transformed into recovered individuals after they eliminated the new coronavirus through autoimmune resistance. The parameter $p_2 > 0$ is the rate at which the asymptomatic individuals become recovered individuals. $\gamma > 0$ is the recovery rate of symptomatic individuals. Clinically, relapse is rare in the cured patients. Thus, in our model, it is assumed that there is no transfer from the recovery individuals to susceptible class. Based on the above assumptions, we formulated an dynamical system (2.1) consisting of four differential equations to depict the flow diagram of COVID-19.

2.1. Model basic properties

To determine the equilibrium points, we set the right-hand side of equations (2.1) to zero and solve the system

$$\begin{cases} 0 = \Lambda - (1-\rho)(\beta_1 E^* + \beta_2 A^* + \beta_3 I^* + \frac{\beta_4 B^*}{K+B^*})S^* - \mu S^*, \\ 0 = (1-\rho)(\beta_1 E^* + \beta_2 A^* + \beta_3 I^* + \frac{\beta_4 B^*}{K+B^*})S^* - (\mu+\omega_1+\omega_2)E^*, \\ 0 = \omega_1 E^* - (\mu+\delta+\gamma_1)A^*, \\ 0 = \omega_2 E^* + \delta A^* - (\mu+d+\gamma_2)I^*, \\ 0 = \gamma_1 A^* + \gamma_2 I^* - \mu R^*, \\ 0 = (1-\rho)\varepsilon_1 E^* + (1-\rho)\varepsilon_2 A^* - (\mu_B+\sigma)B^*. \end{cases} \tag{2.2}$$

By using a substitution method, we first obtain

$$E^* = \frac{Q_2 Q_3 I^*}{Q_2\omega_2 + \delta\omega_1} = M_1 I^*, \tag{2.3}$$

$$A^* = \frac{\omega_1 Q_3 I^*}{Q_2\omega_2 + \delta\omega_1} = M_2 I^*, \tag{2.4}$$

$$R^* = \frac{[\gamma_1\omega_1 Q_3 + \gamma_2(Q_2\omega_2 + \delta\omega_1)]I^*}{(Q_2\omega_2 + \delta\omega_1)\mu} = M_3 I^*, \tag{2.5}$$

$$B^* = \frac{(1-\rho)Q_3(\varepsilon_1 Q_2 + \varepsilon_2\omega_1)}{(\mu_B+\sigma)(Q_2\omega_2 + \delta\omega_1)} = M_4 I^*, \tag{2.6}$$

$$S^* = \frac{\Lambda}{\mu} - \frac{Q_1 Q_2 Q_3 I^*}{(Q_2\omega_2 + \delta\omega_1)\mu} = \frac{\Lambda}{\mu} - M_5 I^*, \tag{2.7}$$

where

$$
\begin{aligned}
Q_1 &= \mu + \omega_1 + \omega_2, \\
Q_2 &= \mu + \gamma_1 + \delta, \\
Q_3 &= \mu + d + \gamma_2, \\
M_1 &= \frac{Q_2 Q_3}{Q_2\omega_2 + \delta\omega_1}, \\
M_2 &= \frac{\omega_1 Q_3}{Q_2\omega_2 + \delta\omega_1}, \\
M_3 &= \frac{\gamma_1\omega_1 Q_3 + \gamma_2(Q_2\omega_2 + \delta\omega_1)}{(Q_2\omega_2 + \delta\omega_1)\mu}, \\
M_4 &= \frac{(1-\rho)Q_3(\varepsilon_1 Q_2 + \varepsilon_2\omega_1)}{(\mu_B + \sigma)(Q_2\omega_2 + \delta\omega_1)}, \\
M_5 &= \frac{Q_1 Q_2 Q_3}{(Q_2\omega_2 + \delta\omega_1)\mu}.
\end{aligned}
$$

The total force of infection is denoted by

$$
f(S^*, E^*, A^*, I^*, B^*) = (1-\rho)(\beta_1 E^* + \beta_2 A^* + \beta_3 I^* + \frac{\beta_4 B^*}{K + B^*})S^*.
$$

Substitute (2.3), (2.4), (2.6), and (2.7) into the second equation of (2.2), we obtain

$$
(\frac{\Lambda}{\mu} - M_5 I^*)(B_1 + B_2 I^*)I^* = Q_1 M_1 I^*(K + M_4)I^*, \tag{2.8}
$$

where $B_1 = (1-\rho)[(\beta_1 M_1 + \beta_2 M_2 + \beta_3)K + \beta_4 M_4]$, $B_2 = (1-\rho)(\beta_1 M_1 + \beta_2 M_2 + \beta_3)M_4$.

In fact, (2.8) is equivalent to a cubic equation of the form of

$$
A_0 I^{*3} + A_1 I^{*2} + A_2 I^* = 0. \tag{2.9}
$$

where

$$
\begin{aligned}
A_0 &= B_2 M_5 > 0, \\
A_1 &= B_1 M_5 + Q_1 M_1 M_4 - \frac{\Lambda}{\mu} B_2, \\
A_2 &= Q_1 M_1 K - \frac{\Lambda}{\mu} B_1 = Q_1 M_1 K(1 - R_0), \\
R_0 &= \frac{(1-\rho)\Lambda}{\mu}(\frac{\beta_1}{Q_1} + \frac{\beta_2\omega_1}{Q_1 Q_2} + \frac{\beta_3(Q_2\omega_2 + \delta\omega_1)}{Q_1 Q_2 Q_3} + \frac{\beta_4(1-\rho)(\varepsilon_1 Q_2 + \varepsilon_2\omega_1)}{Q_1 Q_2 K(\mu_B + \sigma)}).
\end{aligned}
$$

Obviously, $I^* = 0$ is one of the solutions of equation (2.10), which means the existence of the disease-free equilibrium. And the endemic equilibrium is the positive solution of

$$
A_0 I^{2*} + A_1 I^* + A_2 = 0. \tag{2.10}
$$

It is easy to see that $A_2 < 0$ when $R_0 > 1$. Hence, the system (2.1) has only one positive equilibrium for $R_0 > 1$, namely, the endemic equilibrium $P^*(S^*, E^*, A^*, I^*, R^*, B^*)$. Here $I^* = \frac{-A_1+\sqrt{A_1^2-4A_0A_2}}{2A_0} > 0$. Conversely, the system (2.1) has only the disease-free equilibrium, namely, $P_0(\frac{\Lambda}{\mu}, 0, 0, 0, 0, 0)$. Here, R_0 is actually the basic reproduction number of infectious disease model. In the following part, we have a detailed solution process for the basic reproduction number R_0. Mathematical epidemiology has a threshold value, namely the basic reproduction number, to preliminarily predict the outbreak trend of diseases. We can find some key strategies to prevent and control disease spread by surveying their effect on R_0. Next, we will use the next-generation matrix approach to compute the basic reproduction number R_0.

Following [17], the next generation matrix is defined by FV^{-1}. Here, the matrices F and V representing the new infection terms and the remaining transfer terms are respectively given by

$$F = \begin{bmatrix} (1-\rho)\beta_1\frac{\Lambda}{\mu} & (1-\rho)\beta_2\frac{\Lambda}{\mu} & (1-\rho)\beta_3\frac{\Lambda}{\mu} & (1-\rho)\beta_4\frac{\Lambda}{K\mu} \\ 0 & 0 & 0 & 0 \\ 0 & 0 & 0 & 0 \\ 0 & 0 & 0 & 0 \end{bmatrix},$$

$$V = \begin{bmatrix} Q_1 & 0 & 0 & 0 \\ -\omega_1 & Q_2 & 0 & 0 \\ -\omega_2 & -\delta & Q_3 & 0 \\ -(1-\rho)\varepsilon_1 & -(1-\rho)\varepsilon_2 & 0 & \mu_B+\sigma \end{bmatrix}.$$

The basic reproduction number of is now given by

$$R_0 = \rho(FV^{-1}) = R_1 + R_2 + R_3 + R_4,$$

where

$$\begin{aligned} R_1 &= \frac{\Lambda(1-\rho)}{\mu}\frac{\beta_1}{Q_1}, \\ R_2 &= \frac{\Lambda(1-\rho)}{\mu}\frac{\beta_2\omega_1}{Q_1Q_2}, \\ R_3 &= \frac{\Lambda(1-\rho)}{\mu}\frac{\beta_3(Q_2\omega_2+\delta\omega_1)}{Q_1Q_2Q_3}, \\ R_4 &= \frac{\Lambda(1-\rho)}{\mu}\frac{\beta_4(1-\rho)(\varepsilon_1Q_2+\varepsilon_2\omega_1)}{Q_1Q_2K(\mu_B+\sigma)}. \end{aligned}$$

Obviously, The basic reproduction number consists of four parts. Each part R_1, R_2, R_3, and R_4, characterizes the contribution of close contacts, symptomatic infectious, asymptomatic infectious and environment in the process of COVID-19, respectively.

In this section, we focus on the stability of equilibriums of system (2.1). We have the following result on the local asymptotic stability of the disease-free equilibrium P_0.

Theorem 2.1. *The disease-free equilibrium P_0 of the system(2.1) is locally asymptotically stable if $R_0 \leq 1$ and unstable $R_0 > 1$.*

Proof. The Jacobian matrix of the system (2.1) at the disease-free equilibrium P_0 is

$$J(P_0) = \begin{bmatrix} -\mu & -(1-\rho)\beta_1\frac{\Lambda}{\mu} & -(1-\rho)\beta_2\frac{\Lambda}{\mu} & -(1-\rho)\beta_3\frac{\Lambda}{\mu} & 0 & -(1-\rho)\beta_4\frac{\Lambda}{K\mu} \\ 0 & (1-\rho)\beta_1\frac{\Lambda}{\mu} - Q_1 & (1-\rho)\beta_2\frac{\Lambda}{\mu} & (1-\rho)\beta_3\frac{\Lambda}{\mu} & 0 & (1-\rho)\beta_4\frac{\Lambda}{K\mu} \\ 0 & \omega_1 & -Q_2 & 0 & 0 & 0 \\ 0 & \omega_2 & \delta & -Q_3 & 0 & 0 \\ 0 & 0 & \gamma_1 & \gamma_2 & -\mu & 0 \\ 0 & (1-\rho)\varepsilon_1 & (1-\rho)\varepsilon_2 & 0 & 0 & -(\mu_B+\sigma) \end{bmatrix},$$

The Jacobian matrix $J(P_0)$ has eigenvalues $\lambda_1 = \lambda_2 = -\mu$.
The remaining 4×4 submatrix is given as

$$J_1(P_0) = \begin{bmatrix} (1-\rho)\beta_1\frac{\Lambda}{\mu} - Q_1 & (1-\rho)\beta_2\frac{\Lambda}{\mu} & (1-\rho)\beta_3\frac{\Lambda}{\mu} & (1-\rho)\beta_4\frac{\Lambda}{K\mu} \\ \omega_1 & -Q_2 & 0 & 0 \\ \omega_2 & \delta & -Q_3 & 0 \\ (1-\rho)\varepsilon_1 & (1-\rho)\varepsilon_2 & 0 & -(\mu_B+\sigma) \end{bmatrix}.$$

Further, we define

$$B_{11} = Q_1 - (1-\rho)\beta_1\frac{\Lambda}{\mu},\ B_{12} = (1-\rho)\beta_2\frac{\Lambda}{\mu},\ B_{13} = (1-\rho)\beta_3\frac{\Lambda}{\mu},\ B_{14} = (1-\rho)\beta_4\frac{\Lambda}{K\mu},$$
$$B_{21} = \omega_1,\ B_{22} = Q_2,$$
$$B_{31} = \omega_2,\ B_{32} = \delta,\ B_{33} = Q_3,$$
$$B_{41} = (1-\rho)\varepsilon_1,\ B_{42} = (1-\rho)\varepsilon_2,\ B_{44} = \mu_B + \sigma.$$

Then, the remaining submatrix $J_1(P_0)$ can be rewritten as

$$J_1(P_0) = \begin{bmatrix} -B_{11} & B_{12} & B_{13} & B_{14} \\ B_{21} & -B_{22} & 0 & 0 \\ B_{31} & B_{32} & -B_{33} & 0 \\ B_{41} & B_{42} & 0 & -B_{44} \end{bmatrix}.$$

The remaining eigenvalues are the roots of

$$\lambda^4 + C_3\lambda^3 + C_2\lambda^2 + C_1\lambda + C_0 = 0, \tag{2.11}$$

where

$$C_0 = B_{11}B_{22}B_{33}B_{44}(1 - \tfrac{R_2+R_3+R_4}{1-R_1}) + 2B_{13}B_{31}B_{22}B_{44},$$
$$C_1 = B_{11}B_{22}B_{33}(1 - \tfrac{R_2+R_3}{1-R_1}) + B_{11}B_{22}B_{44}(1 - \tfrac{R_4}{1-R_1}) + B_{11}B_{33}B_{44}(1 - \tfrac{R_{41}}{1-R_1}),$$
$$+B_{22}B_{33}B_{44}(1-R_2) + 2B_{22}B_{13}B_{31} + B_{13}B_{31}B_{44},$$
$$C_2 = B_{22}(B_{33}+B_{44}) + B_{33}(B_{11}+B_{44}) + B_{13}B_{31} + B_{11}B_{22}(1-R_2) + B_{11}B_{44}(1-R_{41}),$$
$$C_3 = B_{11} + B_{22} + B_{33} + B_{44} > 0.$$

According to the Routh-Hurwitz stability criterion, we should proof that

$$C_0 > 0,\ C_1 > 0,\ C_2 > 0,\ C_3 > 0. \tag{2.12}$$

$$\begin{aligned}
&\Delta_1 = C_3 > 0,\\
&\Delta_2 = \begin{vmatrix} C_3 & 1 \\ C_1 & C_2 \end{vmatrix} = C_2C_3 - C_1 > 0,\\
&\Delta_3 = \begin{vmatrix} C_3 & 1 & 0 \\ C_1 & C_2 & C_3 \\ 0 & C_1 & C_2 \end{vmatrix} = C_1C_2C_3 - C_1^2 - C_0C_3^2 > 0,\\
&\Delta_4 = \begin{vmatrix} C_3 & 1 & 0 & 0 \\ C_1 & C_2 & C_3 & 1 \\ 0 & C_0 & C_1 & C_2 \\ 0 & 0 & 0 & C_0 \end{vmatrix} = C_0(C_1C_2C_3 - C_1^2 - C_0C_3^2) = C_0\Delta_3 > 0.
\end{aligned} \tag{2.13}$$

When $R_0 \leq 1$, it is obvious that $R_1 < 1$, $R_2 < 1$, $R_3 < 1$, $R_4 < 1$, $R_5 < 1$. It also implies that $C_1 > 0$, $C_2 > 0$, $C_2 > 0$, $\Delta_1 > 0$, $\Delta_2 > 0$, $C_2C_3 > 2C_1$ and $C_1C_2 > 2C_0$ hold.

$$\begin{aligned}
&\Delta_1 = C_3 > 0,\\
&\Delta_2 = B_{11}^2[B_{22}(1-R_2)B_{33}) + B_{33} + B_{44}] + B_{22}^2[B_{11}(1-R_2) + B_{33} + B_{44}]\\
&\quad + B_{33}^2(B_{11} + B_{22} + B_{44}) + B_{44}^2[B_{11}(1-R_{41}) + B_{22} + B_{33}]\\
&\quad + B_{11}B_{22}B_{33}(2-R_2) + B_{11}B_{22}B_{44}(2-R_2-R_{41}) + B_{11}B_{33}B_{44}(2-R_{41})\\
&\quad + 2B_{22}B_{33}B_{44} + B_{13}B_{31}(B_{11} + B_{33}) + B_{14}B_{41}(B_{22} + B_{33})\\
&\quad + B_{21}(B_{14}B_{42} + B_{12}B_{44} + B_{12}B_{33} + B_{13}B_{32}) > 0,
\end{aligned}$$

$$\begin{aligned}
C_1C_2 - 2C_0C_3 = {} & B_{22}B_{33}[B_{11}B_{22}B_{33}(1 - \tfrac{R_2+R_3}{1-R_1}) + B_{22}B_{33}B_{44}(1-R_2) + 2B_{22}B_{13}B_{31}]\\
& + B_{22}B_{44}[B_{11}B_{22}B_{44}(1 - \tfrac{R_4}{1-R_1}) + B_{22}B_{33}B_{44}(1-R_2)]\\
& + B_{11}B_{33}[B_{11}B_{22}B_{33}(1 - \tfrac{R_2+R_3}{1-R_1}) + B_{11}B_{33}B_{44}(1 - \tfrac{R_{41}}{1-R_1}) + B_{13}B_{31}(2B_{22} + B_{44})]\\
& + B_{33}B_{44}[B_{11}B_{33}B_{44}(1 - \tfrac{R_{41}}{1-R_1}) + B_{22}B_{33}B_{44}(1-R_2) + B_{13}B_{31}B_{44}]\\
& + B_{11}B_{22}(1-R_2)[B_{11}B_{22}B_{33}(1 - \tfrac{R_2+R_3}{1-R_1}) + B_{11}B_{22}B_{44}(1 - \tfrac{R_4}{1-R_1}) + 2B_{22}B_{13}B_{31}]\\
& + B_{13}B_{31}[B_{11}B_{33}B_{44}(1 - \tfrac{R_{41}}{1-R_1}) + 2B_{22}B_{13}B_{31} + B_{13}B_{31}B_{44}]\\
& + B_{11}B_{44}(1-R_{41})[B_{11}B_{22}B_{44}(1 - \tfrac{R_4}{1-R_1}) + B_{11}B_{33}B_{44}(1 - \tfrac{R_{41}}{1-R_1}) + B_{13}B_{31}B_{44}]\\
& + B_{11}^2B_{22}B_{33}B_{44}[\tfrac{(1-R_1)+R_3(1-R_2-R_{41})+R_2+R_{41}(R_1+R_2)}{1-R_1} + \tfrac{R_4}{1-R_1}(1 - \tfrac{R_3}{1-R_1})]\\
& + B_{13}B_{21}B_{44}(2B_{22}B_{32} + 3B_{32}B_{44}) + B_{11}B_{22}B_{33}B_{44}^2\tfrac{(1-R_3-R_{41})+R_2+R_{42}+R_2R_{41}}{1-R_1}\\
& + B_{11}B_{22}^2B_{33}B_{44}\tfrac{(1-R_1-R_2-R_3)+R_2^2(1-R_1)+2R_1R_2+R_4}{1-R_1}\\
& + B_{11}B_{22}B_{33}^2B_{44}\tfrac{(1-R_1)(1-R_2)+(R_2+R_{42}+R_4)+R_3(1-R_2)}{1-R_1},
\end{aligned}$$

$$\begin{aligned}
C_2C_3 - 2C_1 = {} & B_{11}^2[B_{22}(1-R_2) + B_{33} + B_{44}] + B_{22}^2[B_{11}(1-R_2) + B_{33} + B_{44}]\\
& + B_{33}^2(B_{11} + B_{22} + B_{44}) + B_{44}^2[B_{11}(1-R_{41}) + B_{22} + B_{33}]\\
& + B_{11}B_{22}B_{33}\tfrac{(1-R_1-R_3)+R_2(1+R_1)}{1-R_1}\\
& + B_{11}B_{22}B_{44}\tfrac{(1-R_1-R_2)+R_1(R_1+R_2)+R_{42}+R_4}{1-R_1}\\
& + B_{11}B_{33}B_{44}\tfrac{(1-R_1-R_3)+R_{41}(1-R_1)}{1-R_1} + B_{22}B_{33}B_{44}(1+2R_2)\\
& + B_{13}B_{31}(B_{11} + B_{33}) + 3B_{13}B_{21}B_{32} > 0,
\end{aligned}$$

where

$$
\begin{aligned}
R_{31} &= \frac{\Lambda(1-\rho)}{\mu}\frac{\beta_3\omega_2}{Q_1Q_3},\\
R_{32} &= \frac{\Lambda(1-\rho)}{\mu}\frac{\beta_3\delta\omega_1}{Q_1Q_2Q_3},\\
R_{31} + R_{32} &= R_3,\\
R_{41} &= \frac{\Lambda(1-\rho)}{\mu}\frac{\beta_4(1-\rho)\varepsilon_1}{Q_1K(\mu_B+\sigma)},\\
R_{42} &= \frac{\Lambda(1-\rho)}{\mu}\frac{\beta_4(1-\rho)\varepsilon_2\omega_1}{Q_1Q_2K(\mu_B+\sigma)},\\
R_4 &= R_{41} + R_{42}.
\end{aligned}
$$

When $R_0 \leq 1$, it is obvious that $R_1 < 1$, $R_2 < 1$, $R_3 < 1$, $R_4 < 1$, $R_5 < 1$. It also implies that $C_1 > 0$, $C_2 > 0$, $C_2 > 0$, $\Delta_1 > 0$, $\Delta_2 > 0$, $C_2C_3 > 2C_1$ and $C_1C_2 > 2C_0$ hold. According to $C_2C_3 > 2C_1$ and $C_1C_2 > 2C_0$, we get $C_1C_2C_3 > \max\{2C_1^2, 2C_0C_3^2\} > C_1^2 + C_0C_3^2$. Therefore, $\Delta_3 > 0$ and $\Delta_4 > 0$.

To sum up, all conditions of Hurwitzs criterion (2.12) and (2.13) hold. Then, the disease-free equilibrium P_0 is local stability for $R_0 \leq 1$. The theorem also implies that influx of a small number of COVID-19 cases will not generate a a large-scale outbreak when the $R_0 \leq 1$. □

In the section, we will discuss the global stability of the disease-free equilibrium and the endemic equilibrium by using comparison theorem and Lyapunov function, respectively. The main results are presented in the Theorem 2.2 and 2.3.

Theorem 2.2. *The disease-free equilibrium P_0 of the system* (2.1) *is globally asymptotically stable if $R_0 \leq 1$.*

Proof. In the system (2.1), the rate of change of the variables describing the infected components can be rewritten as

$$
\begin{bmatrix} \frac{dE}{dt} \\ \frac{dA}{dt} \\ \frac{dI}{dt} \\ \frac{dB}{dt} \end{bmatrix} = (F-V)\begin{bmatrix} E \\ A \\ I \\ B \end{bmatrix} - \begin{bmatrix} C_{11} & C_{12} & C_{13} & C_{14} \\ 0 & 0 & 0 & 0 \\ 0 & 0 & 0 & 0 \\ 0 & 0 & 0 & 0 \end{bmatrix}\begin{bmatrix} E \\ A \\ I \\ B \end{bmatrix}.
$$

where $C_{11} = (1-\rho)\beta_1(\frac{\Lambda}{\mu} - 1) > 0$, $C_{12} = (1-\rho)\beta_2(\frac{\Lambda}{\mu} - 1) > 0$, $C_{13} = (1-\rho)\beta_3(\frac{\Lambda}{\mu} - 1) > 0$, $C_{14} = (1-\rho)\beta_4(\frac{\Lambda}{K\mu} - \frac{1}{K+B}) > 0$. Hence, it can be obtained

$$
\begin{bmatrix} \frac{dE}{dt} \\ \frac{dA}{dt} \\ \frac{dI}{dt} \\ \frac{dB}{dt} \end{bmatrix} \leq (F-V)\begin{bmatrix} E \\ A \\ I \\ B \end{bmatrix}.
$$

In Theorem 2.1, it has been obtained that all eigenvalues of the matrix $F - V$ have negative real parts. And the disease-free equilibrium P_0 is stable when $R_0 \leq 1$. Furthermore, by comparison theorem, it follows that $(E^*, A^*, I^*, B^*) \to (0, 0, 0, 0)$ as $t \to \infty$ [18]. The second, third, fourth, and the sixth equations of (2.2) give $S^* = \frac{\Lambda}{\mu}$ and $R^* = 0$ when $E^* = A^* = I^* = R^* = B^* = 0$. Thus, $(S^*, E^*, A^*, I^*, R^*, B^*) \to (\frac{\Lambda}{\mu}, 0, 0, 0, 0, 0)$ as $t \to \infty$ for $R_0 \leq 1$.

Hence, the disease free equilibrium point P_0 is globally asymptotically stable. □

Next, we analyse global properties of the endemic equilibrium.

Theorem 2.3. *The endemic equilibrium P^* of the system (2.1) is globally asymptotically stable in Ω when $R_0 > 1$ provided that*

$$\begin{array}{llll} \frac{A}{A^*} \leq \frac{f(S,A)}{f(S,A^*)} \leq 1 & for\ all & 0 < A \leq A^*, & and \\ \frac{A}{A^*} \geq \frac{f(S,A)}{f(S,A^*)} \geq 1 & for\ all & A \geq A^*. & \end{array} \tag{2.14}$$

Proof. First, we construct the Lyapunov function

$$V = S - \int_{\epsilon}^{S} \frac{f(S^*,A^*)}{f(\tau,A^*)} d\tau + E - E^* \ln E + \frac{Q_1}{\omega_1}(A - A^* \ln A), \tag{2.15}$$

where $f(S, A) = (\lambda_P + \lambda_B)S$. Similar to $f(S, I)$ in reference [19], $f(S, A)$ is monotonically growing with respect to S and A. Besides, at the endemic equilibrium P^* have

$$\begin{array}{llll} f(S,A^*) < f(S^*,A^*) & for\ all & 0 < S \leq S^*, & and \\ f(S,A^*) > f(S^*,A^*) & for\ all & S < S^*, & \end{array} \tag{2.16}$$

and (2.14).

Derivative (2.15) with respect to time is given by

$$\begin{aligned} \frac{dV}{dt} = {} & \Lambda - \mu S - f(S,A) - \frac{f(S^*,A^*)}{f(S,A^*)}(\Lambda - \mu S - f(S,A)) \\ & + f(S,A) - Q_1 E - \frac{E^*}{E}(f(S,A) - Q_1 E) \\ & + \frac{Q_1}{\omega_1}(\omega_1 E - Q_2 A) - \frac{Q_1 E^*}{\omega_1 E}(\omega_1 E - Q_2 A) \end{aligned} \tag{2.17}$$

We noted that the endemic equilibrium $P^*(S^*, E^*, A^*, I^*, R^*, B^*)$ satisfies (2.2). Then, substituting (2.2) into (2.17) and simplifying can get

$$\begin{aligned} \frac{dV}{dt} = {} & -\mu S^*(1 - \frac{S}{S^*})(1 - \frac{f(S^*,A^*)}{f(S,A^*)}) \\ & + f(S^*,A^*)[4 - \frac{f(S^*,A^*)}{f(S,A^*)} - \frac{E^* f(S,A)}{E f(S^*,A^*)} - \frac{EA^*}{E^* A} - \frac{Af(S,A^*)}{A^* f(S,A)}] \\ & + f(S^*,A^*)[\frac{Af(S,A^*)}{A^* f(S,A)} - 1 - \frac{A}{A^*} + \frac{f(S,A)}{f(S,A^*)}] \end{aligned} \tag{2.18}$$

By (2.14) and (2.16), we can get $\frac{dV}{dt} \leq 0$. It is easy to see that $\frac{dV}{dt} = 0$ holds only when $S = S^*, E = E^*, A = A^*, I = I^*, R = R^*, B = B^*$ in the system (2.1). And P^* is the only equilibrium in Ω. Therefore, by Lyapunov Lasalle asymptotic stability theorem, the equilibrium P^* is globally asymptotically stable in Ω. □

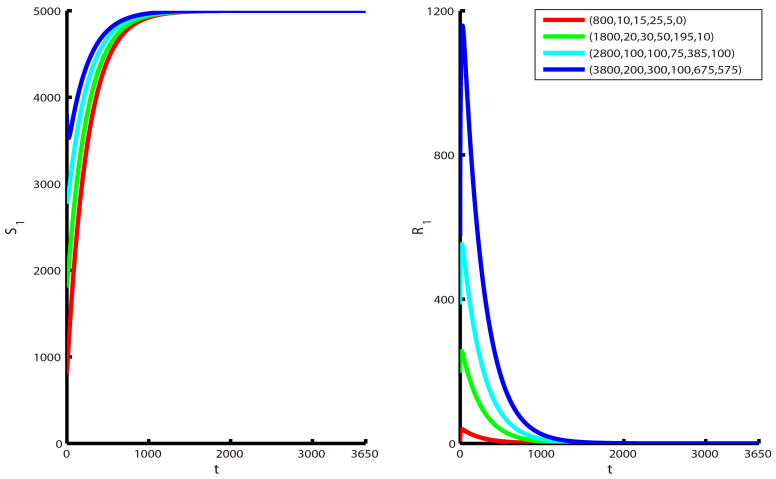

Figure 2: Simulation trajectories starting from different initial values when $R_0 = 0.7072 < 1$. A: The trajectory of the susceptible. B: The trajectory of the recovered.

3. Numerical Simulations

In this section, we firstly focus on the numerical solution of equations (2.1) to validate the previous analysis results obtained. The values and sources of parameters used for simulation are shown in Table 1.

Figure 2 verifies that all numerical solutions from different initial values of equations (2.1) converge to the disease free equilibrium point $P_0(\frac{\Lambda}{\mu}, 0, 0, 0, 0, 0)$ when $R_0 < 1$. And Figure 3 shows that all numerical solutions from different initial values of equations (2.1) converge to the endemic equilibrium point $P^*(S^*, E^*, A^*, I^*, R^*, B^*)$ when $R_0 > 1$. These results are consistent with those discussed in Theorem 2.2 and Theorem 2.3. Further more, we simulate the effects of implementing different control strategies on the susceptible and recovered.

Considering, different countries have different economic levels, so that the sanitary sanitation conditions are also significantly different. We first simulate the impact of simply improving the public health environment on the susceptible and recovered. Figure 3 shows that when the sanitation induced mortality increases 0 to 6, the number of susceptible was increased, but the number of recovered was reduced. It implies that improving environmental sanitation conditions can reduce the risk of infection among susceptible people.

Next, we investigate the impact of health education on the system under the premise of a stable treatment level. Figure 5 plots the time series curve of susceptible and recovery when the health education efficacy parameter the system increases from 0 to 0.8. The result shows that the number of susceptible was significantly increased, but the number of recovery was reduced. And when the health education efficacy parameter reaches 0.8, the number of susceptible in the system initially rises, and finally stabilizes to a higher level. This indicates that the effective implementation of health education, that is, raising everyone's

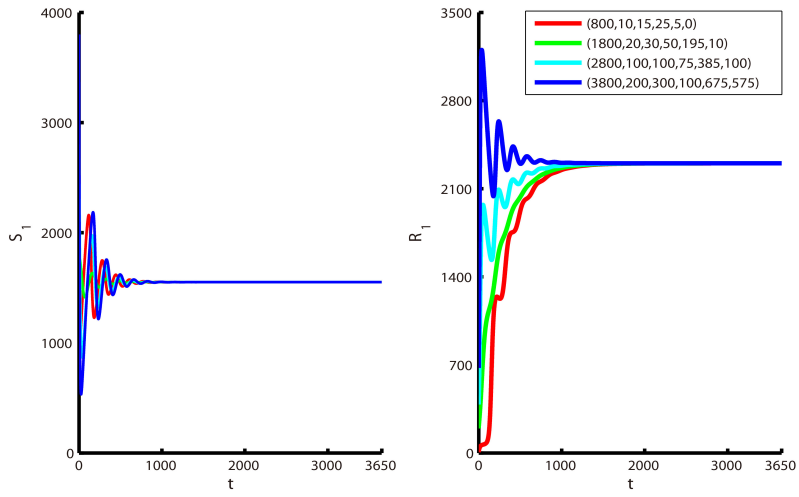

Figure 3: Simulation trajectories starting from different initial values when $R_0 = 3.2232 > 1$. A: The trajectory of the susceptible. B: The trajectory of the recovered.

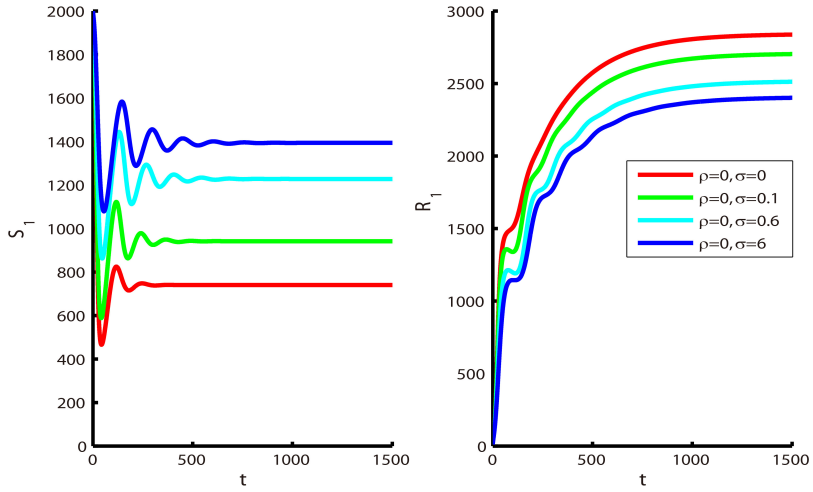

Figure 4: Effect of improving the public sanitation on the susceptible and recovered. A: The trajectory of the susceptible. B: The trajectory of the recovered.

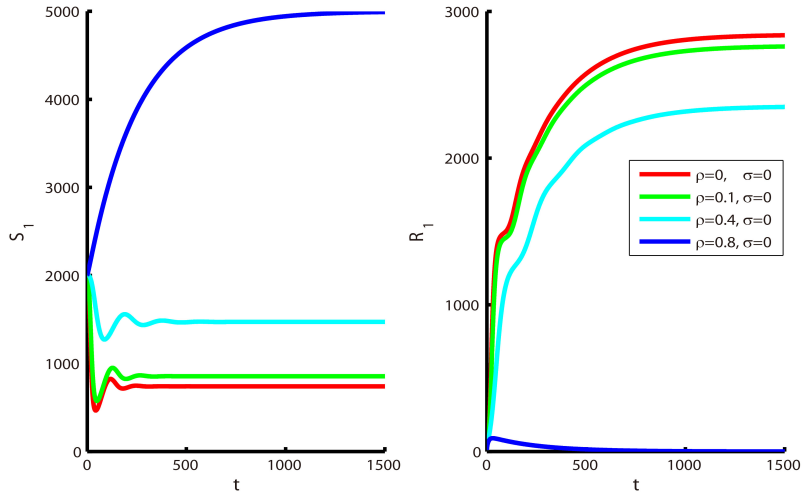

Figure 5: Effect of improving the health education on the susceptible and recovered. A: The trajectory of the susceptible. B: The trajectory of the recovery.

health awareness and prevention awareness can effectively curb the large-scale spread of diseases among the population.

Finally, we simulate the impact of joint implementation of health education and improvement of public sanitation on the system. Figure 6 plots the time series curve of susceptible and recovered when the health education efficacy parameter increases from 0 to 0.8 and the public sanitation induced mortality increases from 0 to 6. The simulation results are similar to Figure 5. However, the joint implementation of these two interventions can effectively control the disease within a controllable range in a more timely manner, and even effectively curb the outbreak of the disease.

In addition, we used a 3D plots look at the topological nature of two parameters(ie. ρ and σ). Figure gives the surface relation of ρ and σ on I^* and R_0. Figure 7A gives the health education and sanitation on the basic reproduction number R_0 using parameter values in Table 1. Numerical results in Figure 7B shows that the increased of health education or sanitation results in a reduce of R_0. But, increasing the values of these two parameters at the same time, the basic reproductionnumber R_0 declined the fastest. It also implies that health education and sanitation has positive impact on the reduction of COVID-19 virus transmission.

Conclusion

A mathematical model of COVID-19 considering health education and public sanitation is presented. The existence and stability of the system steady state have discussed. The results show that the system always has a disease-free equilibrium point. And it is globally asymptotically stable when the basic reproduction number $R_0 \leqq 1$. When the basic reproduction number $R_0 > 1$, the endemic equilibrium point exists and is globally asymptotically

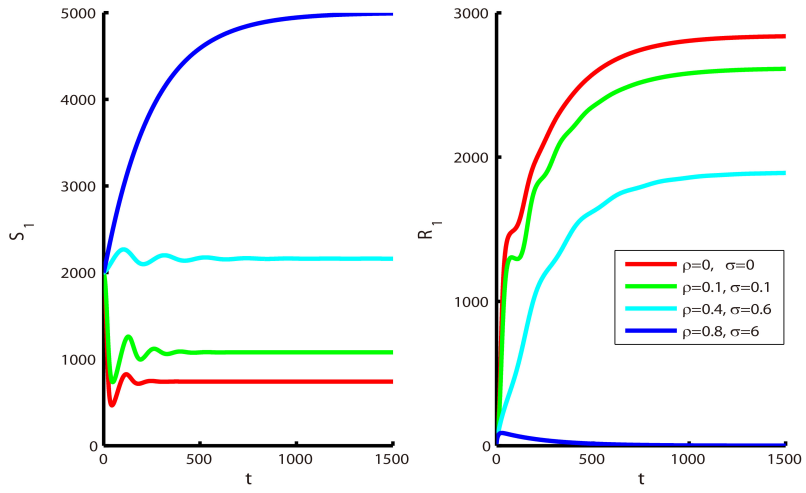

Figure 6: The impact of dual control strategies on the susceptible and recovered. Here, the dual control strategies: health education (ρ) and sanitation(σ). A: The trajectory of the susceptible. B: The trajectory of the recovered.

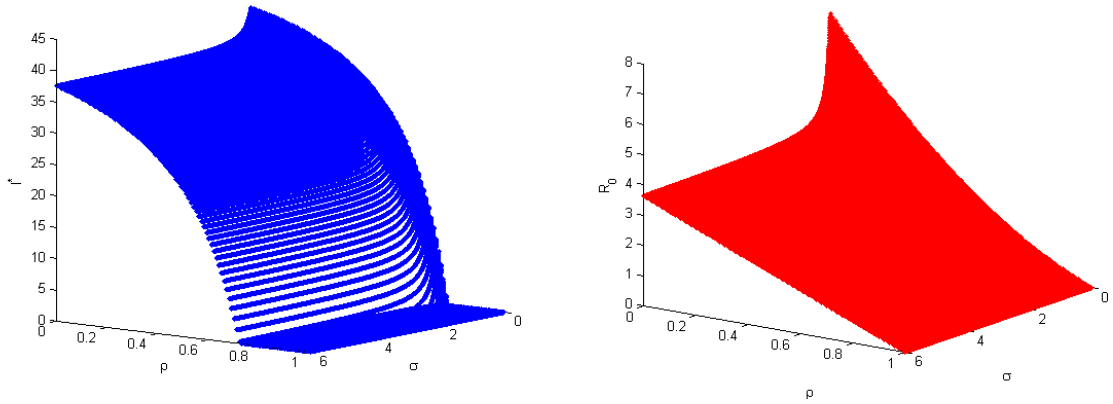

Figure 7: Three dimensional plots of endemic state I^* and R_0. A: Surface plot of endemic state I^* with respect to ρ and σ. B: Surface plot of R_0 with respect to ρ and σ.

stable. Number simulation results indicate that an increase in the efficacy parameter of health education and the mortality rate inducing sanitation may result in the increase of the number susceptible. It implies that the effective way to reduce the spread of the COVID-19 virus is to educate people to raise awareness of prevention and improve the public health environment conditions.

The model presented in this paper is not completely realistic. But it captures some main properties in the COVID-19 infection models. For instance, in order to make the model more realistic, the model considers two modes of transmission, namely direct transmission caused by direct contact between people, and indirect transmission caused by people contacting the environment or objects contaminated by the new coronavirus. In the next step, we will be more interested in the impact of overseas import, vaccination and virus mutation on future epidemics.

Acknowledgment

The authors wish to thank the anonymous reviewers for their careful reading and providing invaluable suggestions. This work was supported by the NSFC under Grant No. 12261070, the Scientific and Technological Innovation Programs of Higher Education Institutions in Shanxi under grant No. 2021L563, the Fundamental Research Program of Shanxi Province under grant No. 202103021224317, and The present job was also partially supported by School Research Project of Anhui University of Finance and Economics, grant No. ACKYC21049.

CRediT authorship contribution statement

Xiaxia Kang: Conceptualization, Methodology, Visualization, Writing - original draft. **Fang Cheng**: Investigation, Formal analysis, Funding acquisition, Writing - review & editing.

Declaration of Competing Interest

The authors declare that there is no conflict of interests.

ORCID

Fang Cheng: https://orcid.org/0000-0002-4368-1518

References

[1] B. Tang, X. Wang, Q. Li, et al. Estimation of the Transmission Risk of the 2019-nCoV and Its Implication for Public Health Interventions. J Clin Med. 9(2): 462, 2020.

[2] N. R. Sasmita, M. Ikhwan, S. Suyanto, et al. Optimal control on a mathematical model to pattern the progression of coronavirus disease 2019 (COVID-19) in Indonesia. Glob Health Res Policy. 5: 38, 2020.

[3] K. Liang. Mathematical model of infection kinetics and its analysis for COVID-19, SARS and MERS. Infect Genet Evol. 82: 104306, 2020.

[4] F. Ndairou, I. Area, J. J. Nieto, et al. Mathematical modeling of COVID-19 transmission dynamics with a case study of Wuhan. Chaos Solitons Fractals. 135:109846, 2020.
[5] M. Mandal, S. Jana, S.K. Nandi, et al. A model based study on the dynamics of COVID-19: Prediction and control. Chaos Solitons Fractals. 136: 109889, 2020.
[6] Z. Hu, Y. Wu, M. Su, et al. Population migration, spread of COVID-19, and epidemic prevention and control: empirical evidence from China. BMC Public Health. 21(1): 529, 2021.
[7] T. M. Chen, J. Rui, Q. P. Wang, et al. A mathematical model for simulating the phase-based transmissibility of a novel coronavirus. Infect Dis Poverty. 9(1): 24, 2020.
[8] R. Sommerstein, C. A. Fux, D. Vuichard-Gysin, et al. Risk of SARS-CoV-2 transmission by aerosols, the rational use of masks, and protection of healthcare workers from COVID-19. Antimicrob Resist Infect Control. 9(1): 100, 2020.
[9] D. S. Saputri, S. Li, F. J. van Eerden, et al. Flexible, Functional, and Familiar: Characteristics of SARS-CoV-2 Spike Protein Evolution. Front Microbiol. 11: 2112, 2020.
[10] D. M. Teli, M. B. Shah, M.T. Chhabria. In silico Screening of Natural Compounds as Potential Inhibitors of SARS-CoV-2 Main Protease and Spike RBD: Targets for COVID-19. Front Mol Biosci. 7: 599079, 2021.
[11] D. E. Gordon, J. Hiatt, M. Bouhaddou, et al. Comparative host-coronavirus protein interaction networks reveal pan-viral disease mechanisms. Science. 370(6521): eabe9403, 2020.
[12] A. Ather, B. Patel, N.B. Ruparel, et al. Coronavirus Disease 19 (COVID-19): Implications for Clinical Dental Care. J Endod. 46(5): 584-595, 2020.
[13] Y. Y. Zuo, W. E. Uspal, T. Wei. Airborne Transmission of COVID-19: Aerosol Dispersion, Lung Deposition, and Virus-Receptor Interactions. ACS Nano. acsnano.0c08484, 2020.
[14] J. Cai, W. Sun, J. Huang , et al. Indirect Virus Transmission in Cluster of COVID-19 Cases, Wenzhou, China, 2020. Emerg Infect Dis. 26(6): 1343-1345, 2020.
[15] W. J. Guan, Z. Y. Ni, Y. Hu, et al. China Medical Treatment Expert Group for Covid-19. Clinical Characteristics of Coronavirus Disease 2019 in China. N Engl J Med. 382(18): 1708-1720, 2020.
[16] Z. Hu, C. Song, C. Xu, et al. Clinical characteristics of 24 asymptomatic infections with COVID-19 screened among close contacts in Nanjing, China. Sci China Life Sci. 63(5): 706-711, 2020.
[17] J. B. Aguilar, J. B. Gutierrez. An Epidemiological Model of Malaria Accounting for Asymptomatic Carriers. Bull Math Biol. 82(3): 42, 2020.
[18] N. Shaban. Modelling the Effects of Public Health Education in the Spread of Hepatitis Bdisease. Applied Mathematical Sciences. 9: 3967-3981, 2015.
[19] A. Korobeinikov. Global properties of infectious disease models with nonlinear incidence. Bull Math Biol. 69(6): 1871-86, 2007.